

# Surface-Induced *J* Aggregation of Pseudoisocyanine Dye at a Glass/Solution Interface Studied by Total-Internal-Reflection Fluorescence Spectroscopy

Hiroshi Yao, Hiroshi Ikeda, and Noboru Kitamura\*

Division of Chemistry, Graduate School of Science, Hokkaido University, Kita-ku, Sapporo 060-0810, Japan

Received: June 30, 1998; In Final Form: August 10, 1998

An aqueous pseudoisocyanine dye solution in a soda lime glass optical cell exhibited the new absorption band of a *J* aggregate at around 577 nm ( $J_L$  aggregate) at room temperature. The  $J_L$  band was slightly red-shifted and broader (hwhm:  $\sim 130\text{ cm}^{-1}$ ) compared to the previously reported *J* band ( $J_S$  band; peak,  $\sim 572\text{ nm}$ ; hwhm,  $\sim 70\text{ cm}^{-1}$ ). Since formation of the  $J_L$  aggregate was not observed in a quartz glass cell, it was concluded that  $J_L$  aggregate formation was induced by interactions between the dye and the soda lime glass surface. Total-internal-reflection fluorescence spectroscopy proved that the  $J_L$  aggregate was distributed only in the vicinity of the glass surface, whereas the  $J_S$  aggregate was produced in the bulk water phase.

## Introduction

In concentrated aqueous dye solutions, a spectral shift or appearance of a new absorption band is often observed owing to formation of dimers or higher-order aggregates of the dye.<sup>1,2</sup> As a typical example, it is well-known that 1,1'-diethyl-2,2'-cyanine halide (pseudoisocyanine halide; PIC) forms so-called *J* aggregates at a high dye concentration and/or low temperature, showing intense and very narrow excitonic absorption (*J* band) in the longer wavelength compared to the maximum peak of the relevant monomer band.<sup>3–5</sup> Recently, *J* aggregates have attracted considerable attention as molecular assemblies for a system bridging the gap between the physics of a single molecule and structurally ordered crystals or that for optical communications based on their high nonlinear optical coefficients.<sup>6</sup>

So far, several models for the molecular structure of the *J* aggregate have been proposed: a threadlike structure on a scale of hundreds of nanometers or a ribbonlike structure on a molecular level.<sup>7–9</sup> The absorption line shape of the *J* aggregate has been also studied, and it has been reported that the sharpness of the optical transition can be explained by motional narrowing, indicating that the inhomogeneous line profile becomes narrow by a factor of a square root of the coherent size of the aggregate through delocalization of excitation.<sup>10</sup> It has been also suggested more precisely that the line shape is influenced by a disorder parameter, which implies deviation of the distribution of molecular transition energies.<sup>11</sup> It has been reported, however, that motional narrowing would be not so important for determining the line shape of a PIC aggregate, since the diagonal disorder of the molecular energy levels is highly correlated even in a single aggregate.<sup>9</sup> The morphologies of the *J* aggregates of PIC in polymer films have been also discussed on the basis of near-field scanning optical microscopy.<sup>12–14</sup> It demonstrated that the molecules within the aggregate were highly ordered on a nanometer dimensional scale, and energy migration in the aggregate was limited to less than  $\sim 50\text{ nm}$ .

Despite such experimental and theoretical studies, definite structures of the *J* aggregate including the aggregation number and its morphology have been poorly understood and are controversial, since factors governing the structures and characteristics of the *J* aggregate such as structural dimension, effects

of a counteranion, lattice defects, and an aggregate size distribution are still ambiguous. For instance, the *J* band of a pseudoisocyanine dye (PIC) shows a slightly different absorption maximum ( $\lambda_{\text{max}}$ ), depending on the nature of a counteranion of the dye as demonstrated in a solution phase or LB films.<sup>5,8,15–17</sup> Concentrated aqueous PIC-Cl (chloride) solutions ( $>10\text{ mM}$ ) show  $\lambda_{\text{max}}$  of the *J* band at  $\sim 572\text{ nm}$ , whereas PIC-Br (bromide) and PIC-I (iodide) precipitate before *J* aggregates formation at room temperature.<sup>8</sup> In water/ethylene glycol glasses at 77 K, PIC-I shows the *J* band at  $\lambda_{\text{max}} = 576\text{ nm}$  while PIC-Br exhibits two closely spaced narrow bands at 572 and 578 nm.<sup>5,15–17</sup> These results suggest formation of structurally different dye aggregates depending on experimental conditions. In monolayer LB films, furthermore, it has been reported that a PIC-Br/stearic acid or/dihexadecyl phosphate system at room temperature shows  $\lambda_{\text{max}}$  of the *J* band at 578 or 569 nm, respectively.<sup>18</sup>

Previous studies demonstrated that an aqueous PIC-Cl solution at room temperature showed an intense *J* band at  $\sim 572\text{ nm}$  above  $\sim 10\text{ mM}$ .<sup>3–5</sup> In the course of spectroscopic measurements of the *J* aggregate in aqueous PIC-Cl solutions at room temperature, however, we found a new absorption band at around 577 nm in addition to the reported band at around 572 nm. It is worth emphasizing that the new *J* band at 577 nm can be found in an optical cell made of a soda lime glass but not in a conventional quartz glass cell, suggesting surface-induced aggregation of PIC-Cl in solution. As an analogous study, although it has been reported that *J* aggregation of thiacyanocyanine dyes is caused by adsorption of the dye on potassium sulfate or dipotassium tartrate crystals, its detailed mechanisms and the role of surface adsorption in *J* aggregate formation are still unresolved.<sup>19,20</sup> To elucidate characteristics of the new *J* band and its surface-induced phenomenon, therefore, we explored total-internal-reflection (TIR) fluorescence spectroscopy in addition to conventional absorption spectroscopy.<sup>21</sup> In this Letter, we report explicit evidence of surface-induced formation of the PIC-Cl *J* aggregate and show depth concentration profiles of both new (577 nm) and previously known (572 nm) *J* aggregates, and demonstrate that TIR fluorescence analyses are highly potential for studying *J* aggregate formation in minute space.

## Experimental Section

**Chemicals.** 1,1'-Diethyl-2,2'-cyanine chloride (pseudoisocyanine; PIC) was obtained from Nippon Kankoh-Shikiso Kenkyusho Co. and used as received. Pure water was obtained by an Aquarius GSR-200 (Advantec Co. Ltd.). Soda lime glass (S-1111; Matsunami Glass Industries, Ltd.) and quartz glass plates (Fujiwara Ltd.) used for optical cells were dried at 300 and 500 °C, respectively. Major components of the soda lime glass used were SiO<sub>2</sub> (70%), Na<sub>2</sub>O (12%), CaO (6.5%), K<sub>2</sub>O (4%), and ZnO (4%).

**Measurements.** Conventional absorption spectroscopy was performed with a Hitachi U-3300 spectrophotometer. A thin-layer optical cell was prepared by adhering two glass plates with an aluminum foil being used as a thin spacer (~25 μm). A TIR fluorescence spectroscopy system used in this study was similar to that reported in ref 21. Briefly, a fused silica hemicylindrical prism was contacted with a thin-layer optical (soda lime or quartz glass) cell with *cis/trans*-decaline (Wako Pure Chemicals) being used as a matching oil, and was firmly mounted on a rotating stage (Chuo Seiki). The refractive indices of the prism, the matching oil, the soda lime glass and the aqueous solution are 1.458, 1.475, 1.52, and 1.33, respectively.<sup>22</sup> An Ar<sup>+</sup> laser beam (Coherent, Innova 70, 514.5 nm) passed through a pinhole (400 μm) was used for excitation (~1 mW) and perpendicularly polarized with respect to the reflection plane. The beam was impinged to the thin-layer cell/sample solution interface with an angle of incidence  $\theta_i$  normal to the interface. Fluorescence from the sample passed through a sharp-cut filter (Toshiba Glass,  $\lambda > 530$  nm) was introduced to an optical fiber set at an angle  $\theta_0$  (observation angle) and analyzed with a polychromator-multichannel photodetector (PMA-11, Hamamatsu Photonics) set. The angle between the incident laser beam and the optical fiber was fixed at 90° throughout the experiments, and, thus,  $\theta_0$  equals (90° -  $\theta_i$ ). The performance of the present TIR system was checked by rhodamine B (0.3 mM) in water or ethylene glycol as a standard sample.<sup>21</sup>

## Simulation of the Incident Angle Dependence of the TIR Fluorescence Intensity

In a TIR regime, when an incident angle  $\theta_i$  is larger than a critical angle  $\theta_c$ , incident light is totally reflected at a solid/liquid interface, but an evanescent wave propagates into the interface region of the sample. Thus, information about a solid/liquid interface can be obtained by observing fluorescence under the TIR conditions. In such a case, the observed fluorescence intensity,  $I_f$ , is given by<sup>23</sup>

$$I_f = E_0^2 \frac{4n_1^2 \cos^2 \theta_i}{(n_1 \cos \theta_i + \text{Re})^2 + \text{Im}^2} \cdot \frac{4n_1^2 \cos^2 \theta_0}{[n_1 \cos \theta_0 + (n_2^2 - n_1^2 \sin^2 \theta_0)^{0.5}]^2} \times \int_0^L \epsilon \cdot C \cdot \exp\left(-\frac{4\pi \text{Im} z}{\lambda_0}\right) dz \quad (1)$$

where  $n$  is a refractive index (the suffices 1 and 2 indicate a glass substrate and a sample layer, respectively) and  $E_0$  and  $\lambda_0$  are the electric-field amplitude and the wavelength of incident light, respectively.  $L$ ,  $\epsilon$ , and  $C$  represent the thickness of a sample layer, the molar extinction coefficient at  $\lambda_0$ , and the concentration of a probe molecule, respectively. When a sample solution absorbs incident light, the relevant refractive index is given by a complex number:  $n_2 = n_2(1 + i\kappa)$ , where  $\kappa$  is the

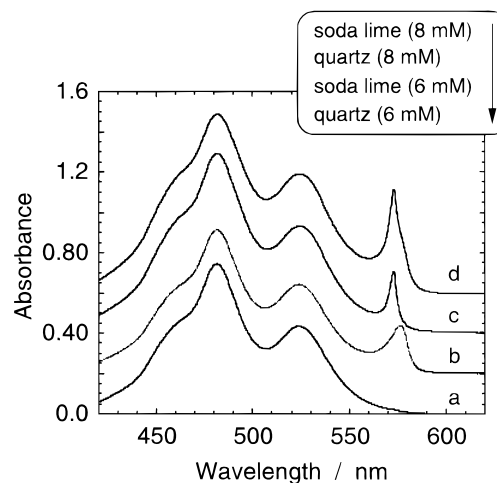


**Figure 1.** Absorption spectra of aqueous pseudoisocyanine (PIC) solutions in soda lime (b and d) and quartz glass cells (a and c). The optical path length of the cell was set to ~25 μm.

absorption index of a probe molecule. The values  $\text{Re}$  and  $\text{Im}$  in eq 1 are the real and imaginary parts of  $(n_2 \cos \theta_i)$ , where  $\theta_i$  is defined as a complex refraction angle<sup>23</sup> and is a function of  $n_1$ ,  $n_2$ ,  $\theta_i$ , and  $\kappa$ . In eq 1, an observation volume determined by an observation angle  $\theta_0$  is provided by the reciprocal law.<sup>24</sup>

When a sample is a homogeneous solution,  $C$  is constant. If a sample has a concentration gradient normal to the TIR element/solution interface ( $z$ -axis), on the other hand, an absorption effect of incident light by a sample on  $I_f$  must be considered. As the first approximation, we assume that  $C$  is given as an exponential function,

$$C = C_0 \exp(-hz) \quad (2)$$

where  $C_0$  and  $h$  represent the concentration of the sample solution at the solid/liquid interface and the position (along the  $z$ -axis) from the interface, respectively. Introducing eq 2 into eq 1, one can evaluate a concentration gradient of the sample in the vicinity of the interface on the basis of a simulation of an incident angle dependence of  $I_f$  by eqs 1 and 2 with  $\kappa$  and  $h$  as parameters.

## Results and Discussion

**Absorption Spectroscopy.** Figure 1 shows absorption spectra of aqueous PIC solutions (6 and 8 mM) observed in a quartz or soda lime glass cell. For a 6 mM solution in a quartz cell (part a, in Figure 1), the monomer and dimer bands were observed at 525 and 480 nm, respectively, whereas a sharp  $J$  band (bandwidth:  $\Delta\nu \sim 70$  cm<sup>-1</sup>, hwhm) was also observed at ~572 nm for an 8 mM solution (c); the well-known  $J$  aggregate is abbreviated as  $J_S$ . When a soda lime glass cell was used, on the other hand, a slightly broad  $J$  band ( $\Delta\nu \sim 130$  cm<sup>-1</sup>) was observed at 577 nm even for a 6 mM solution (b). To the best of our knowledge, this  $J$  band abbreviated as  $J_L$  was found for the first time in an aqueous PIC solution. It is clear that the  $J_L$  aggregate is different from  $J_S$  since both peak position and bandwidth are different from each other. For an 8 mM solution in a soda lime glass cell (d), although formation of  $J_S$  is facilitated and the intense peak of the  $J_S$  band is observed, the  $J_L$  band is also observed as a longer-wavelength shoulder of the  $J_S$  band. Thus,  $J_L$  formation is characteristic to the soda lime glass surface, and  $J_S$  formation is concentration dependent. Different from the composition of a quartz glass, a soda lime glass involves considerable amounts of exchangeable ions such

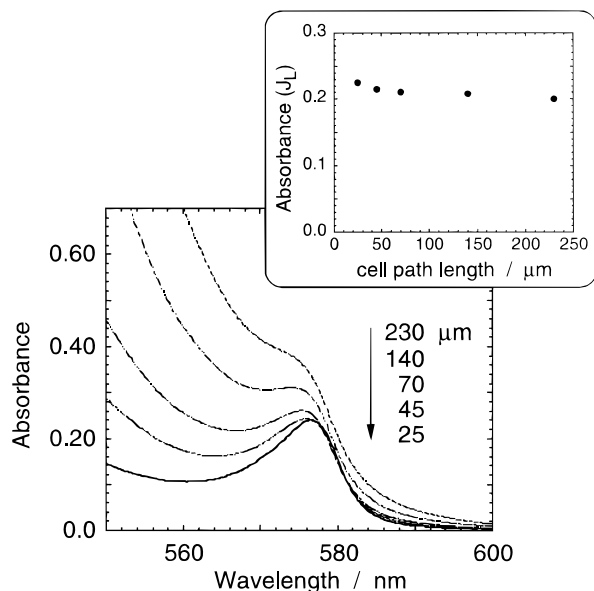


**Figure 2.** Optical path length dependence of the absorption spectrum of an aqueous PIC solution (6 mM, soda lime glass cell). The inset shows a cell path length dependence on the  $J_L$  absorbance.

as  $\text{Na}^+$ ,  $\text{Ca}^{2+}$ , and  $\text{K}^+$ , so that the  $J_L$  formation is supposed to be induced by anionic sites on the soda lime glass surface.<sup>18,25</sup> The surface- and anion site-induced  $J_L$  aggregate formation is also supported by the fact that analogous results with those in a soda lime glass cell can be observed in a BK 7 borosilicate glass cell containing exchangeable ions ( $\text{Na}_2\text{O}$  (8.8%),  $\text{K}_2\text{O}$  (8.4%)).

Figure 2 shows an optical path length dependence of the absorption spectrum of an aqueous PIC (6 mM) solution, determined in soda lime glass cells. Optical absorption at the wavelength shorter than 560 nm is due to that by the monomer, and the absorbance increased linearly with an increase in the optical path length. Subtracting the contribution of monomer absorption, an optical path length dependence of the absorbance of the  $J_L$  band at 577 nm was determined as shown in the inset of Figure 2. It is clear that the absorbance of the  $J_L$  band is essentially independent of the path length. Thus, it can be concluded that formation of the  $J_L$  aggregate is confined to the vicinity of the glass surface. Furthermore, although the  $J_L$  formation was confirmed above  $\sim 0.5$  mM, the absorbance at 577 nm was saturated at  $\geq \sim 4$  mM (data are not shown here). The results indicate quasi-adsorption of the  $J_L$  aggregate onto the glass/solution interface.

**TIR Fluorescence Spectroscopy.** The  $J_L$  aggregate formation is induced by the surface properties of the soda lime glass and confined to the vicinity of the surface, while the  $J_S$  aggregate is produced homogeneously in the cell as suggested by the increase in the absorbance with an increase of the PIC concentration (Figure 2). To obtain clear evidence for this, we explored TIR fluorescence spectroscopy. Figure 3 shows TIR fluorescence spectra of PIC (6 or 8 mM) under several conditions. The critical angles for TIR ( $\theta_c$ ) at the soda lime glass/solution or quartz glass/solution interface is  $\sim 61^\circ$  or  $\sim 66^\circ$ , respectively, so that excitation at the incident angle of  $\theta_i = 51^\circ$  or  $77^\circ$  can monitor bulk or TIR fluorescence of PIC, respectively.

In a soda lime glass cell (8 mM), the fluorescence bands responsible for the  $J_S$  and  $J_L$  aggregates were observed at around 573 and 580 nm, respectively. As clearly seen in Figure 3a, however, the spectrum was strongly dependent on  $\theta_i$ . At  $\theta_i = 51^\circ (<\theta_c)$ , namely, the  $J_S$  band is more intense than the  $J_L$  band,

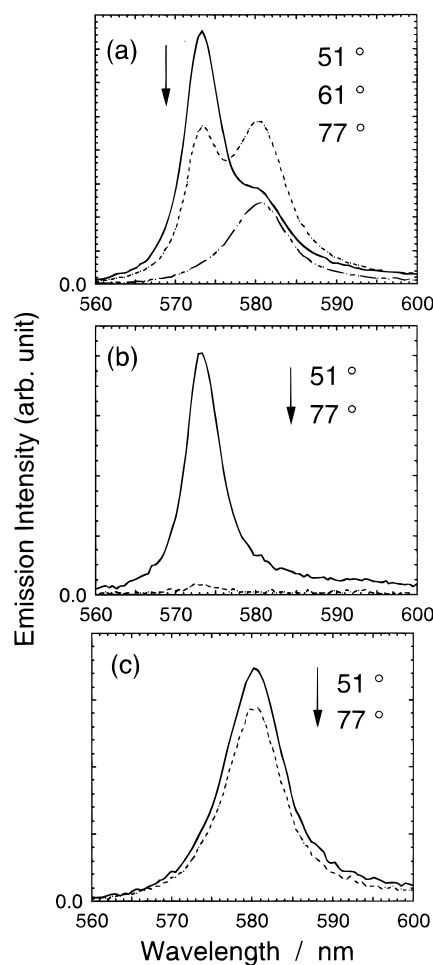


**Figure 3.** Total-internal-reflection (TIR) fluorescence spectra of aqueous PIC solutions in soda lime and quartz glass cells: (a) 8 mM, soda lime glass; (b) 8 mM, quartz glass; (c) 6 mM, soda lime glass,

while the main contribution to the spectrum at  $\theta_i = 77^\circ (>\theta_c)$  is the  $J_L$  band. The change in the relative contribution of the  $J_L$  and  $J_S$  fluorescence to the observed spectrum with  $\theta_i$  indicates clearly that the spatial distributions of the aggregates in the sample solution are totally different from each other. The results proved that the  $J_L$  aggregate is produced in the surface layer of the soda lime glass/solution boundary. In a quartz glass cell (8 mM, Figure 3b), on the other hand, the spectrum is characterized by  $J_S$  fluorescence irrespective of  $\theta_i$ , demonstrating that the  $J_S$  aggregate is produced almost homogeneously in the cell. For a 6 mM solution in a soda lime glass cell (Figure 3c), contrarily, the spectrum is best characterized by  $J_L$  fluorescence at both  $\theta_i = 51^\circ$  and  $77^\circ$ . The results also demonstrate that the spatial distribution of the  $J_S$  and/or  $J_L$  aggregates in a sample cell is dependent strongly on the nature of the cell and the concentration of PIC.

To elucidate the spatial distributions of the  $J_S$  and  $J_L$  aggregates, therefore, incident angle dependencies of the fluorescence intensities at 573 ( $J_S$ ) and/or 580 nm ( $J_L$ ) were studied, and the results are summarized in Figure 4, where the data shown in parts a, b, and c are relevant to those in Figure 3. In a soda lime glass cell (Figure 4a), strong  $J_S$  fluorescence is observed at  $\theta_i < 61^\circ$ , while its intensity decreases very sharply at around  $\theta_c$  ( $\sim 61^\circ$ ). On the other hand, the fluorescence intensity of the  $J_L$  aggregate increases with increasing  $\theta_i$  from  $\sim 50^\circ$  to  $\sim 61^\circ$ . At  $\theta_i > \theta_c$ , however, the intensity does not decrease sharply, but decreases gradually up to  $\theta_i \sim 80^\circ$  in contrast to the results on the  $J_S$  fluorescence. Analogous results



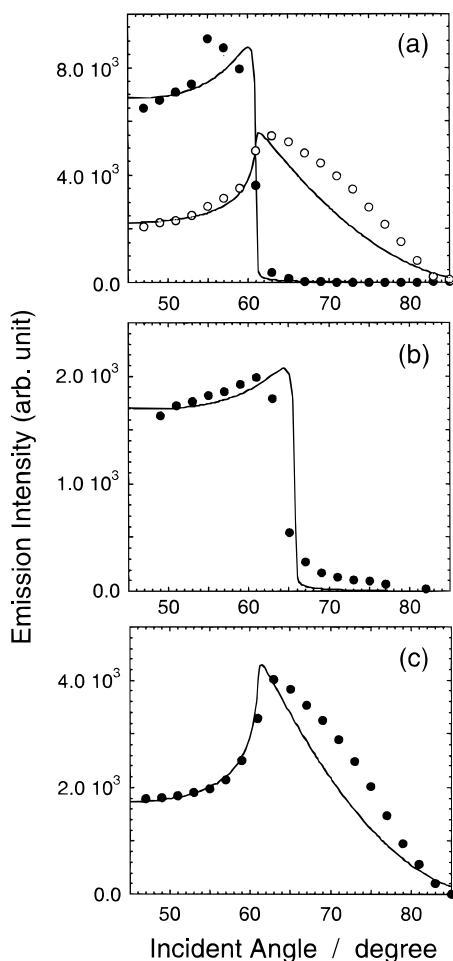


**Figure 4.** Incident angle dependencies of the fluorescence peak intensities for aqueous PIC solutions in soda lime and quartz glass cells: (a) 8 mM, soda lime glass ( $J_S$  emission,  $\bullet$ ;  $J_L$  emission,  $\circ$ ); (b) 8 mM, quartz glass; (c) 6 mM, soda lime glass. The solid curves show the simulated ones (see main text).

with those for  $J_S$  were observed in a quartz cell (Figure 4b), while the  $\theta_i$  dependence of the  $J_L$  fluorescence intensity in a 6 mM/soda lime glass cell (Figure 4c) was similar to that for an 8 mM/soda lime cell (Figure 4a).

The results in Figure 4 involve information about the concentration profiles of the  $J_S$  and  $J_L$  aggregates. Therefore, a simulation of the data was performed with eqs 1 and 2, as shown by the solid curves in the figures. The sharp incident angle profile of the  $J_S$  fluorescence intensity shown in part a or b of Figure 4 was well simulated by an absorption index parameter of  $\kappa_{JS} = 1.5 \times 10^{-4}$  and  $C$  to be constant, indicating that the  $J_S$  aggregate is produced homogeneously in the solution phase. However, the incident angle profile of the  $J_L$  fluorescence intensity was not simulated by assuming a homogeneous distribution of the aggregate. When  $J_L$  produces homogeneously, the fluorescence intensity should change sharply at around  $\theta_i \sim \theta_c$ , similar to that observed for  $J_S$ . However, this is not the case for the present system. We conclude that the  $J_L$  aggregate formation is confined to the glass/solution interface;  $C$  is not a constant. Therefore, a simulation was performed by  $h$  (length from the interface) as a parameter (see eq 2). Although the  $\theta_i$  dependence of the  $J_L$  fluorescence intensity at  $\theta_i < \theta_c$  or  $\theta_i > \theta_c$  was very sensitive to the parameter  $\kappa$  or  $h$ , respectively, the observed data were best simulated with  $\kappa_{JL} = 1.0 \times 10^{-3}$  and  $h = 2$  nm as shown by the solid curves in parts a and c of Figure 4. The simulated curve somewhat underestimates the

observed data at  $\theta_i > \theta_c$ . Although the discrepancy between the observed and simulated data at  $\theta_i > \theta_c$  decreased with decreasing  $h$ , that was constant at  $h \leq 2$  nm. A possible reason for the discrepancy will be an inhomogeneous distribution of the  $J_L$  aggregate on the glass surface, and therefore, the  $h$  value might involve some uncertainty. Nonetheless, it is worth emphasizing that the  $h$  value (2 nm) obtained by the simulation proves explicitly that the  $J_L$  aggregate formation is confined to the surface layer of the soda lime glass, and its thickness is extremely thin as compared to the wavelength of incident light. One might point out that such a thin layer on a surface cannot be resolved by TIR spectroscopy in the visible region. However, since the  $J_L$  aggregate strongly absorbs incident light at 514.5 nm, excitation of the sample is confined to very small volumes on the surface and thus  $h \sim 2$  nm is meaningful.<sup>21,23</sup>

Although further experimental and theoretical study is necessary, the present work demonstrated clearly the surface-induced  $J$  aggregation of PIC on a soda lime glass surface and the important roles of the anion sites. Also, TIR fluorescence spectroscopy proves that the  $J_S$  aggregate is produced homogeneously in the solution phase, while the  $J_L$  aggregate observed for the first time at the absorption peak of 577 nm was confined to the surface layer of the soda lime glass alone. Further properties of the  $J_L$  aggregate on the surface will be elucidated by time-resolved fluorescence spectroscopy, which is in progress in this laboratory.<sup>26</sup>

**Acknowledgment.** N.K. is grateful for a Grant-in-Aid from the Ministry of Education, Science, Sports and Culture (08404051) for partial support of the research.

## References and Notes

- (1) Herz, A. H. *Adv. Colloid Sci.* **1977**, *8*, 237.
- (2) McRae, E. G.; Kasha, M. *J. Chem. Phys.* **1958**, *28*, 721.
- (3) Jelley, E. E. *Nature* **1936**, *138*, 1009; **1937**, *139*, 631.
- (4) Scheibe, G. *Angew. Chem.* **1937**, *50*, 212.
- (5) De Boer, S.; Vink, K. J.; Wiersma, D. A. *Chem. Phys. Lett.* **1987**, *137*, 99.
- (6) Spano, F. C.; Mukamel, S. *Phys. Rev. A* **1989**, *40*, 5783.
- (7) Scherer, P. O. J.; Fischer, S. F. *Chem. Phys.* **1984**, *86*, 269.
- (8) Daltrozzo, E.; Scheibe, G.; Gschwind, K.; Haimel, F. *Photogr. Sci. Eng.* **1974**, *18*, 441.
- (9) Kobayashi, T., Ed. *J. aggregates*; World Scientific: Singapore, 1996.
- (10) Knapp, E. W. *Chem. Phys.* **1984**, *85*, 73.
- (11) Fiddler, H.; Terpstra, J.; Wiersma, D. A. *J. Chem. Phys.* **1991**, *94*, 6895.
- (12) Higgins, D. A.; Barbara, P. F. *J. Phys. Chem.* **1995**, *99*, 3.
- (13) Higgins, D. A.; Reid, P. J.; Barbara, P. F. *J. Phys. Chem.* **1996**, *100*, 1174.
- (14) Higgins, D. A.; Kerimo, J.; Vanden Bout, D. A.; Barbara, P. F. *J. Am. Chem. Soc.* **1996**, *118*, 4049.
- (15) Cooper, W. *Chem. Phys. Lett.* **1970**, *7*, 73.
- (16) Yu, Z. X.; Lu, P. Y.; Alfano, R. R. *Chem. Phys.* **1983**, *79*, 289.
- (17) Sundström, V.; Gillbro, T.; Gadonas, R. A.; Piskarskas, A. *J. Chem. Phys.* **1988**, *89*, 2754.
- (18) Hall, R. A.; Kajikawa, K.; Hara, M.; Knoll, W. *Thin Solid Films* **1997**, *295*, 266.
- (19) Hada, H.; Honda, C.; Tanemura, H. *Photogr. Sci. Eng.* **1977**, *21*, 83.
- (20) Honda, C.; Hada, H. *Photogr. Sci. Eng.* **1977**, *21*, 91.
- (21) Masuhara, H.; DeSchryver, F. C.; Kitamura, N.; Tamai, N., Eds. *Microchemistry: Spectroscopy and Chemistry in Small Domains*; North-Holland: Amsterdam, 1994.
- (22) Lide, D. R., Ed. *CRC Handbook of Chemistry and Physics*, 71st ed.; CRC Press Inc.: Boca Raton, FL, 1990.
- (23) Toriumi, M.; Yanagimachi, M.; Masuhara, H. *Appl. Opt.* **1992**, *31*, 6376.
- (24) Carniglia, C. K.; Mandel, L.; Drexhage, K. H. *J. Opt. Soc. Am.* **1972**, *62*, 479.
- (25) El-Shamy, T. M. *Phys. Chem. Glasses* **1973**, *14*, 18.
- (26) Yao, H.; Ikeda, H.; Kitamura, N. To be submitted.